Journal of Sound and Vibration (2000) **236**(2), 193–207
doi:10.1006/jsvi.1999.2969, available online at http://www.idealibrary.com on IDEAL®

EXPERIMENTAL VERIFICATION OF DYNAMIC STABILITY OF VERTICAL CANTILEVERED COLUMNS SUBJECTED TO A SUB-TANGENTIAL FORCE

Y. SUGIYAMA, K. KATAYAMA AND K. KIRIYAMA

Department of Aerospace Engineering, Osaka Prefecture University, Gakuen-cho, Sakai-shi 599-8531, *Japan. E-mail: sugiyama@aero.osakafu-u.ac.jp*

AND

B.-J. RYU

Department of Mechanical Design Engineering, Taejon National University of Technology, Taejon 300-172, *Korea*

(*Received* 8 *October* 1998, *and in final form* 9 *June* 1999)

The intended aim of the paper is to give the experimental verification of the effect of non-conservative/follower force on the vibration and stability of cantilevered columns. In place of an ideal tangential force, a sub-tangential force produced by a real solid rocket motor is considered in this paper. A solid rocket motor is mounted to a vertical cantilevered column at its tip end. Rocket thrust of the motor produces a tangential/non-conservative force, while the self-weight of the motor a vertical/conservative force. Thus, the combined action of the rocket thrust and the self-weight of the rocket motor produces a sub-tangential force. It is assumed that a solid rocket motor is a rigid body. Therefore, a concentrated mass, a rotary inertia and a size of the rocket motor must be taken into account in vibration and stability analysis. FEM formulation of the vibration problem under consideration is conducted to depict the dynamic stability in the total applied force and the non-conservativeness parameter plane. Experiments were conducted to demonstrate the stabilizing effect of follower forces on the dynamics of vertical columns initially subjected to a conservative force due to the rocket motor's weight. It was assumed that the thrust and the self-weight were constant during the burning time of 4 s. The average thrust was 40 kgf (392 N), while the average dead weight of the motor was 14·2 kgf (139 N). Four test runs were made for sub-critical and critical column initially subjected to the dead weight of the motor. It was observed that the buckled column under the dead weight of the motor could be stabilized dynamically by applying the rocket thrust of 40 kgf, when a resultant compressive force of 54·2 kgf (531 N) was applied to the column.

1. INTRODUCTION

The dynamic stability of elastic columns subjected to a non-conservative/follower force has been the subject of a great deal of interests for structural dynamists in these decades. General aspects of the non-conservative stability problems have been compiled in the book by Bolotin [1].

Through the development of non-conservative stability problems, the relation between the conservative and non-conservative stability problems has been one of the interesting topics. Thus, many papers have been published on the stability of columns under the

0022-460X/00/370193 + 15 $35.00/0

combined action of conservative and non-conservative forces [2–4]. The conservative force can be realized easily by gravity as a dead load or a self-weight of structures. The non-conservative force can be produced as rocket thrust of a solid rocket motor which is mounted to a cantilevered column at its tip [5–7]. The combined action of the two forces makes a subtangential force. During the course of theoretical studies of the stability problems of columns subjected to a subtangential force, it has been predicted that a subtangential force yields a higher critical force than a conservative force [1, 4, 8, 9]. However, so far no experimental evidence has been presented for the effect of the subtangential force on the stability of columns.

Under these circumstances, the intended aim of the present paper is to report the experimental observation of the effect of a subtangential follower force on the stability of vertical cantilevered columns. Self-weight of a solid rocket motor fixed at the tip end of the column makes a conservative loading which acts on the column initially, while a rocket thrust of the motor yields a non-conservative loading which acts on the column in addition to the conservative one, thus the total compressive load is much more greater than the buckling load of the considered column. The present paper describes an experimental observation that application of rocket thrust to a column under the action of critical conservative force can make the column stable dynamically as long as the thrust acts on the column.

It is worthwhile to make a mention of the effect of damping. One of the interesting topics in non-conservative stability problems has been the destabilizing effect of damping [1]. It is noted first that this effect has not been verified experimentally. The destabilizing effect is obtained when the asymptotic stability condition is applied to non-conservative systems. The asymptotic stability condition implies that the dynamical system is unstable if the amplitude of the disturbed motion of the system becomes infinite as the time goes to infinity. However, it is of vital importance to watch the behavior of complex eigenvalues in case of the destabilizing effect of damping. It is found that the most dangerous eigenvalue mostly runs in parallel with the imaginary axis. The growth rate of the amplitude of the motion is thus very small indeed. Mathematically, the asymptotic stability criterion gives the theoretical lower flutter limit when the flutter load is applied for an infinite time interval, however in practice, a follower force caused by a rocket motor can act upon elastic structures only for a finite time interval. In the latter case, the theoretical flutter limit obtained by neglecting damping can predict the experimental flutter limit [7, 8, 10]. This is the reason why the damping is neglected in the following discussions.

2. MATHEMATICAL MODEL

Figure 1 shows a vertical cantilevered column in the experimental set-up designed and built up for the present study. Figure 2 shows a corresponding mathematical counterpart of the column subjected to a combined action of a tangential force T and a vertical force W. The column is assumed to be a slender uniform column. The mass per unit length is denoted by m. EI is the bending stiffness of the column, where E is Young's modulus and I the second moment of inertia of the column. The tangential force T and the vertical one W can be produced, respectively, by the rocket thrust and the dead weight of a rocket motor, which is mounted to the column at its tip end. The rocket motor is considered as a rigid body, not a mass point as it has been assumed in many papers published so far. M is the mass of the rocket motor, J the rotary inertia of the rocket motor, and a means the distance between the free end of the column and the mass center of the rocket motor. Thus, the distance a represents the size of the motor. On the assumption of small deflection, the resultant

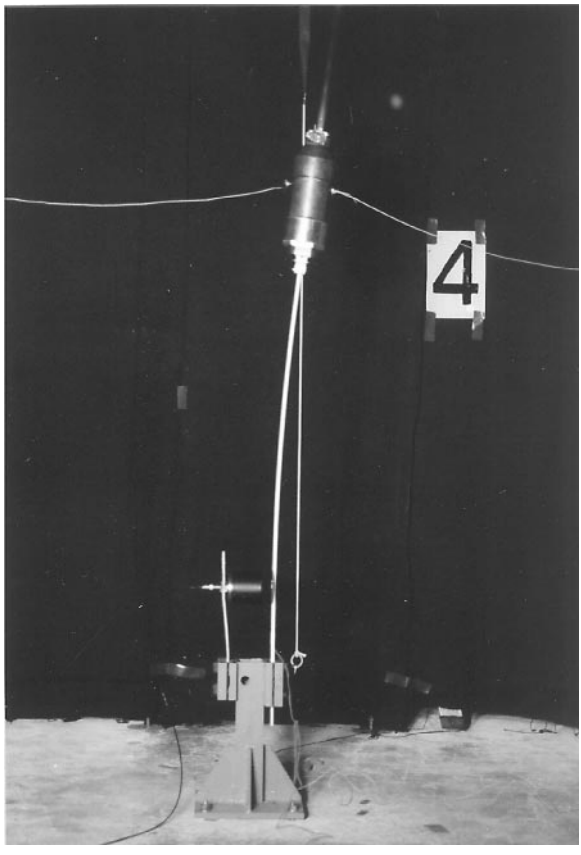

Figure 1. A vertical cantilevered column accommodated with a rocket motor at its tip.

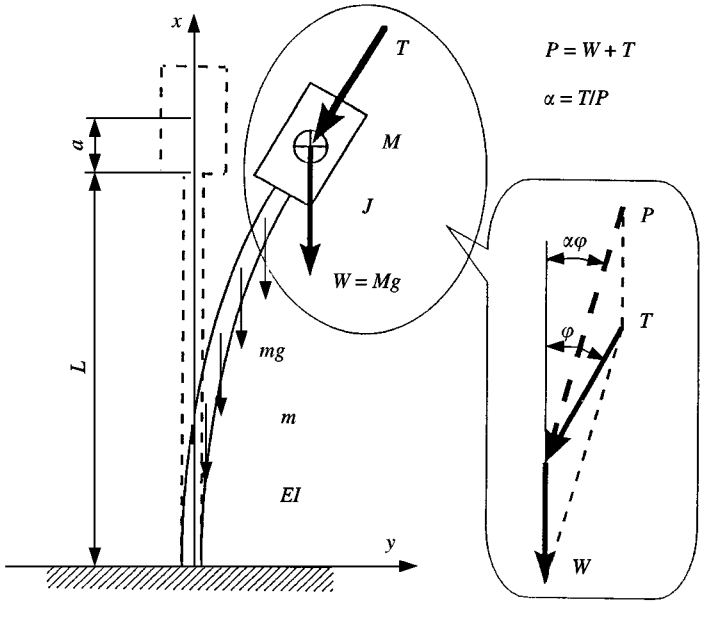

Figure 2. Mathematical model of a vertical cantilevered column.

vector of a vertical force $W\,(=Mg)$ and a pure tangential follower thrust T can make a subtangential force $P\,(=W+T)$. The direction of the resultant subtangential force P is specified by $\alpha\phi$ as shown in Figure 2, where ϕ is the angle of inclination of the tangent at the tip end and assumed to be small ($\phi \ll 1$). The parameter α can specify the angle between the direction of the resultant force and the x-axis, and it is called "tangency coefficient". When $\alpha = 0$, the direction of the force is vertical, i.e., the force is conservative. When $\alpha = 1{\cdot}0$, it is tangential to the tip end, i.e., the force is purely non-conservative. Thus, the coefficient α is sometimes referred to as the non-conservativeness parameter.

3. FORMULATION OF THE PROBLEM

The energy expressions for the above mathematical model are written in the following forms.

The kinetic energy of the uniform column:

$$T_{kc} = \frac{1}{2}\int_0^L m\left(\frac{\partial y}{\partial t}\right)^2 \mathrm{d}x. \tag{1}$$

The kinetic energy of the rocket motor:

$$T_{kr} = \frac{1}{2}M\left[\frac{\partial y}{\partial t} + a\,\frac{\partial}{\partial t}\left(\frac{\partial y}{\partial x}\right)\right]^2_{x=L} + \frac{1}{2}J\left(\frac{\partial^2 y}{\partial t \partial x}\right)^2_{x=L}. \tag{2}$$

The work done by the conservative component of the applied forces:

$$W_c = \frac{1}{2}\int_0^L (W+T)\left(\frac{\partial y}{\partial x}\right)^2 \mathrm{d}x. \tag{3}$$

The work done by the moment due to the dead weight of the motor:

$$W_a = \frac{1}{2}Wa\left(\frac{\partial y}{\partial x}\right)^2_{x=L}. \tag{4}$$

The work done by the distributed self-weight of the uniform column:

$$W_{sw} = \frac{1}{2}\int_0^L mg(L-x)\left(\frac{\partial y}{\partial x}\right)^2 \mathrm{d}x. \tag{5}$$

The virtual work done by the non-conservative component of the rocket thrust:

$$\delta W_{nc} = -T\left(\frac{\partial y}{\partial x}\right)_{x=L}\delta y. \tag{6}$$

The strain energy due to bending:

$$U = \frac{1}{2}\int_0^L EI\left(\frac{\partial^2 y}{\partial x^2}\right)^2 \mathrm{d}x. \tag{7}$$

In order to derive the equation of motion, let us start with the following extended Hamilton's principle:

$$\delta \int_{t_1}^{t_2} (T_{kc} + T_{kr} + W_c + W_a + W_{sw} - U)\,\mathrm{d}t + \int_{t_1}^{t_2} \delta W_{nc}\,\mathrm{d}t = 0. \tag{8}$$

Substitution of equations (1)–(7) into equation (8) leads to

$$\begin{aligned}
&\int_{t_1}^{t_2} \int_0^L \left[m \frac{\partial y}{\partial t}\,\delta\left(\frac{\partial y}{\partial t}\right) + P \frac{\partial y}{\partial x}\,\delta\left(\frac{\partial y}{\partial x}\right) + mg(L-x)\frac{\partial y}{\partial x}\,\delta\left(\frac{\partial y}{\partial x}\right) - EI \frac{\partial^2 y}{\partial x^2}\,\delta\left(\frac{\partial^2 y}{\partial x^2}\right)\right] \mathrm{d}x\,\mathrm{d}t \\
&\quad + \int_{t_1}^{t_2} \left[M \frac{\partial y}{\partial t}\,\delta\left(\frac{\partial y}{\partial t}\right) + J \frac{\partial^2 y}{\partial t \partial x}\,\delta\left(\frac{\partial^2 y}{\partial t \partial x}\right) + Ma \left\{ \frac{\partial y}{\partial t}\,\delta\left(\frac{\partial^2 y}{\partial t \partial x}\right) + \frac{\partial^2 y}{\partial t \partial x}\,\delta\left(\frac{\partial y}{\partial t}\right)\right\}\right. \\
&\quad \left. + Ma^2 \frac{\partial^2 y}{\partial t \partial x}\,\delta\left(\frac{\partial^2 y}{\partial t \partial x}\right) + (1-\alpha) Pa \frac{\partial y}{\partial x}\,\delta\left(\frac{\partial y}{\partial x}\right) - \alpha P \frac{\partial y}{\partial x}\,\delta y \right]_{x=L} \mathrm{d}t = 0,
\end{aligned} \tag{9}$$

where

$$P = W + T, \qquad \alpha = T/P. \tag{10}$$

For simplicity, the following dimensionless quantities are introduced:

$$\begin{aligned}
&\tau = \frac{t}{L^2}\sqrt{\frac{EI}{m}}, \qquad \rho = \frac{PL^2}{EI}, \qquad \beta = \frac{mgL^3}{EI}, \qquad \mu = \frac{M}{mL}, \\
&\nu = \frac{J}{mL^3}, \qquad \gamma = \frac{a}{L}, \qquad \xi = \frac{x}{L}, \qquad \eta = \frac{y}{L}.
\end{aligned} \tag{11}$$

Equation (9) with equation (11) can be written in the dimensionless form as

$$\begin{aligned}
&\int_{t_1}^{t_2} \left[\int_0^L \{\eta_\tau \delta\eta_\tau + \rho\eta_\xi \delta\eta_\xi + \beta(1-\xi)\eta_\xi \delta\eta_\xi - \eta_{\xi\xi}\delta\eta_{\xi\xi}\}\,\mathrm{d}\xi \right. \\
&\quad \left. + \{\mu\eta_\tau \delta\eta_\tau + \mu\gamma\eta_\tau \delta\eta_{\tau\xi} + \mu\gamma\eta_{\tau\xi}\delta\eta_\tau + (\nu + \mu\gamma^2)\eta_{\tau\xi}\delta\eta_{\tau\xi} + (1-\alpha)\rho\gamma\eta_\xi\delta\eta_\xi - \alpha\rho\eta_\xi\delta\eta\}_{\xi=1} \right],
\end{aligned} \tag{12}$$

where differentiation with respect to the non-dimensional independent variables τ and ξ is denoted by the corresponding subscripts.

For discretization of equation (12), the column is divided into N equal finite elements with the shape function of the third order algebraic expressions. Following the ordinary finite element formulation (e.g., see reference [9]), the equation of motion in a matrix form can be obtained in the form

$$\mathbf{M}\mathbf{V}_{\tau\tau} + \mathbf{K}\mathbf{V} = \mathbf{0}, \tag{13}$$

where $\mathbf{M}$ and $\mathbf{K}$ denote the global stiffness matrix and the global mass matrix respectively. $\mathbf{V}$ is the vector of the generalized nodal displacements. The nodal displacement is assumed

to vary with time according to an exponential law in the form

$$\mathbf{V} = \mathbf{V}_0 \exp(\Omega). \tag{14}$$

Finally, the global characteristic equation can be obtained in the form

$$|\mathbf{M}^{-1}\mathbf{K} + \Omega^2\mathbf{E}| = \mathbf{0}, \tag{15}$$

where **E** is the unit matrix.

The stability of the system under consideration is determined by the sign of eigenvalue Ω^2. The stability criterion are as follows.

If $\mathrm{Re}(-\Omega^2) \geqslant 0$ and $\mathrm{Im}(-\Omega^2) = 0$, the system is stable.
If $\mathrm{Re}(-\Omega^2) < 0$ and $\mathrm{Im}(-\Omega^2) = 0$, statically unstable, i.e., divergence-type instability takes place.
If $\mathrm{Re}(-\Omega^2) < 0$ and $\mathrm{Im}(-\Omega^2) \neq 0$, dynamically unstable, i.e., flutter-type instability takes place.

4. ROCKET MOTORS AND TEST COLUMNS

4.1. ROCKET MOTORS

The rocket motors used in the present experiment were small-sized solid rocket motors designed and made by Daicel Chemical Industries, Ltd. for the combustion test of the propellant. This is the reason why the motor is armed by a heavy motor case for safety of the combustion test. The total length of the motor was 344 mm. The mass of the solid rocket motors was measured to find that the nominal initial mass of the motor is 14·65 kg. Initial mass of the rocket motor includes the mass of propellant of 0·9 kg. The average mass of the motor during burning is thus 14·2 kg. The thrust curve of the rocket motor is shown in Figure 3. The average thrust was assumed to be a constant value of 40 kgf (392 N). The rotary inertia of the rocket motor was $J = 0{\cdot}1196\ \mathrm{kg\,m^2}$, and the distance between the center of gravity of the rocket motor and the free end of the column was $a = 200$ mm.

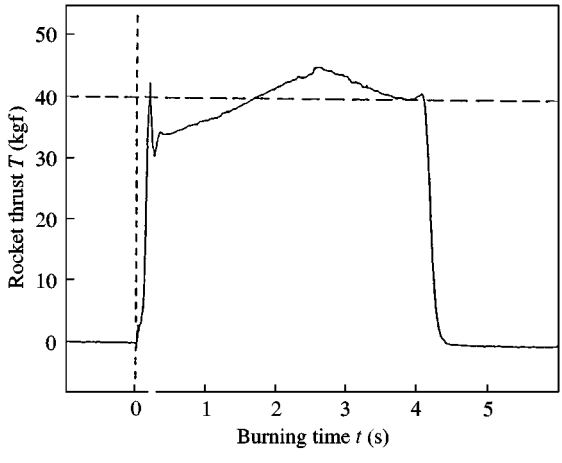

Figure 3. Thrust curve of the rocket motor.

4.2. TEST COLUMNS

Since only four rocket motors were provided, so only four test runs were planned in the present experimental project. Thus, detailed considerations on the design of the test columns were needed. The divergence and flutter forces of the columns having different dimensions are calculated by equation (15) for candidate test columns. Considering that the initial conservative force was 14·65 kgf, the following four test columns were finally designed and made for the planned four test runs:

Test column No. 1: $1040 \times 30 \times 9$ mm,

Test column No. 2: $1130 \times 30 \times 9$ mm,

Test column No. 3: $1330 \times 30 \times 9$ mm,

Test column No. 4: $1125 \times 30 \times 8$ mm.

The columns were made of aluminium with the measured density $\rho = 2672\ \text{kg/m}^3$.

In order to correctly predict instability boundaries by calculation, it is needed to know the bending stiffness EI of the test columns. The bending stiffness EI was obtained by the static bending test of the columns. The experimental bending stiffness EI yielded experimental Young's modulus of test columns: $E = 6{\cdot}90 \times 10^3\ \text{kgf/mm}^2$ (67·6 GPa).

It is noted that all the tests described in the present paper were conducted upon the metric engineering units with the force unit of kgf (kilogram-force). The unit of kgf can be converted into SI force unit of N by the amplification factor of 9·8.

5. NUMERICAL RESULTS

5.1. EIGENFREQUENCY OF TEST COLUMN

To help understanding the dynamics of the columns in the present experiment, the first and second eigenfrequencies of the columns with and without the rocket thrust were calculated by the characteristic equation (15). The frequencies of the columns with and without the rocket thrust for the test column No. 2 are plotted in Figure 4. In Figure 4, points C_1 and C_2 denote the first and second eigenfrequency of the column under no axial loading, respectively. Curve C_1D_1 shows the first eigenfrequency of the column under a conservative loading ($\alpha = 0$), while curve C_1F depicts the frequency under a subtangential loading of $\alpha = 0{\cdot}74$. Knowing the rocket thrust T is assumed to be a constant value of 40 kgf, the tangency coefficient α during the application of the rocket thrust is given by

$$\alpha = 40/(14{\cdot}2 + 40) = 0{\cdot}74, \tag{16}$$

where the average dead weight of the rocket motor during burning is taken as 14·2 kgf, since it was assumed that the initial dead weight of the motor is 14·65 kgf and the weight of the propellant is 0·9 kgf (thus the final dead weight of the motor is 13·75 kg).

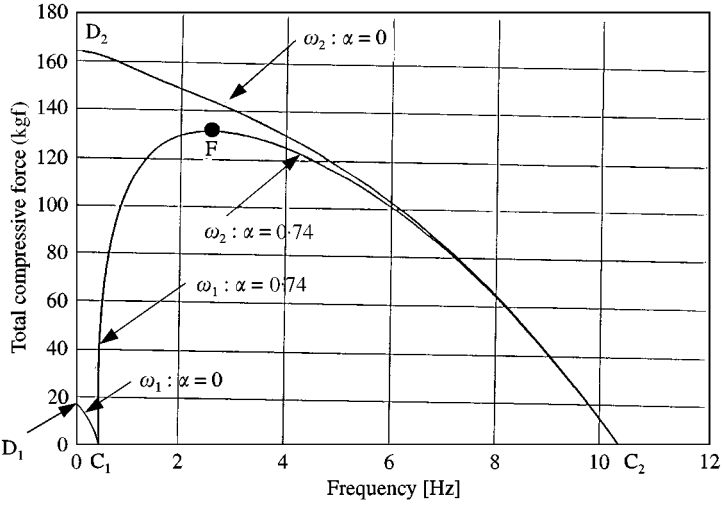

Figure 4. First and second eigenfrequencies for the test column No. 2.

Points D_1 and D_2 in Figure 4 mean the first and second divergence force in case of conservative loading, respectively, while point F represents the flutter point on the eigenvalue curve for $\alpha = 0{\cdot}74$.

5.2. STABILITY MAPS OF THE TEST COLUMNS

Type of instability of the columns depends on the tangency coefficient α of the total compressive force ($P = W + T$). When the tangency coefficient α is changed from zero to unity, the divergence-type instability in the first mode can take place for the coefficient $\alpha \leqslant 0{\cdot}5$, while for $\alpha > 0{\cdot}5$ flutter-type instability can occur. Stability maps of the test columns are shown in Figures 5–8. It is noted that the distributed self-weight (mg) of the

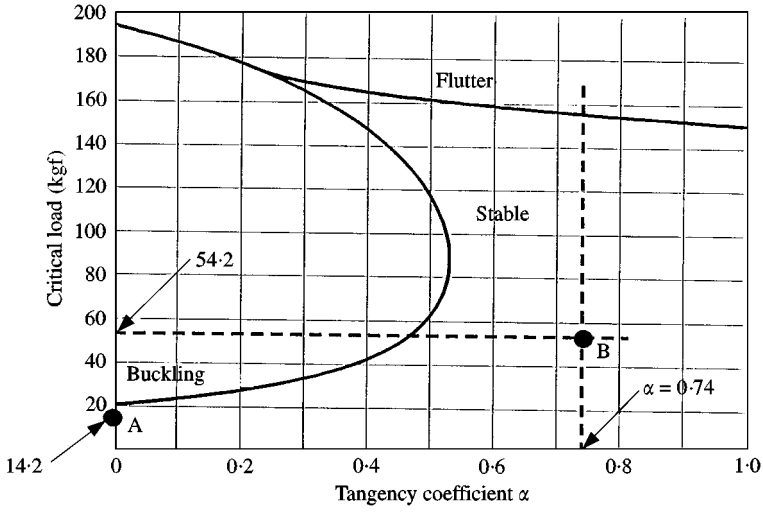

Figure 5. Stability map for the test column No. 1.

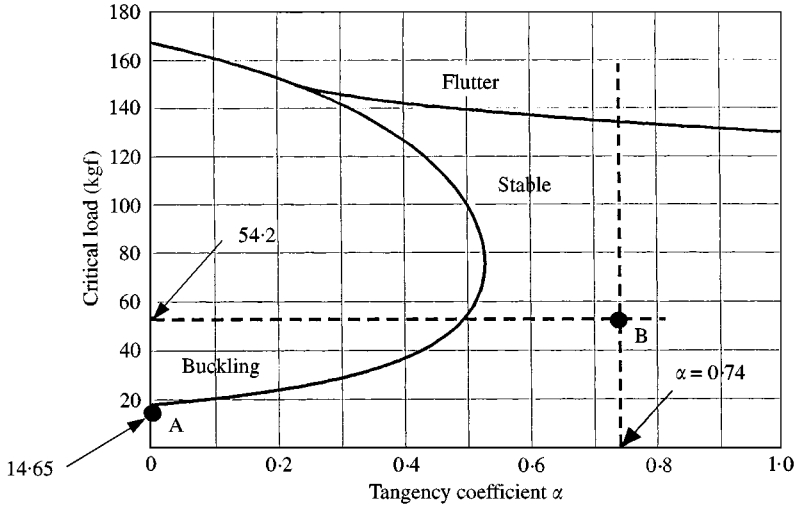

Figure 6. Stability map for the test column No. 2.

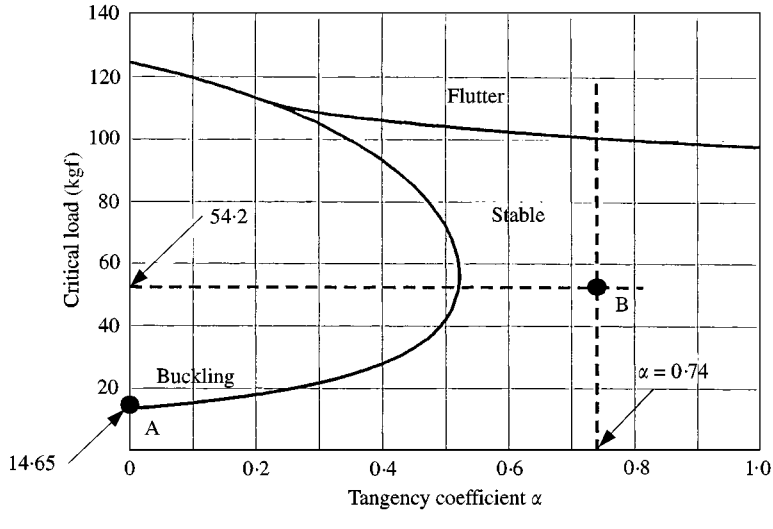

Figure 7. Stability map for the test column No. 3.

uniform columns has no significant effect on the dynamics and stability of the present test columns.

6. EXPERIMENT WITH ROCKET THRUST

6.1. OUTLINE OF THE EXPERIMENT

The purpose of the present experiment is to demonstrate the stabilizing effect of rocket thrust on the dynamics of vertical cantilevered columns, which are initially subjected to

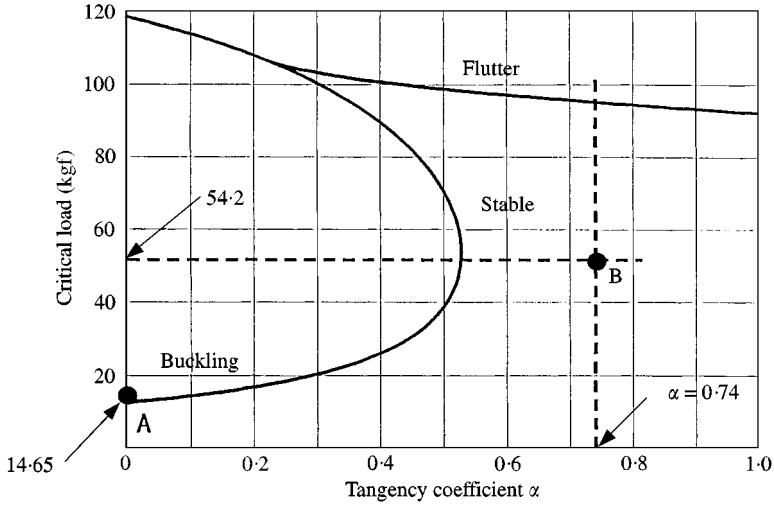

Figure 8. Stability map for the test column No. 4.

a conservative force. As seen in Figure 4, the first eigenfrequency decreases as the conservative load ($\alpha = 0$) increases, while it increases slightly as the subtangential load of $\alpha = 0{\cdot}74$ increases. It is now confirmed that the term "stabilizing" effect here implies "higher" frequency. Four stability maps in Figures 5–8 depict in a straightforward way the state of stability of the columns when they were subjected to (1) a conservative load of $\alpha = 0$ and (2) then to a subtangential load of $\alpha = 0{\cdot}74$. In Figures 5–8, point A means the column under a conservative load ($\alpha = 0$), while point B the column under a subtangential load of $\alpha = 0{\cdot}74$. When the tangency coefficient $\alpha = 0$, the column may lose its stability by divergence, i.e., buckling. When the coefficient $\alpha = 0{\cdot}74$, the column can lose its stability by flutter. It is noted that the flutter load is much more higher than the divergence one, as seen by Figures 4 and 5–8. Application of a rocket thrust to the column in addition to a conservative load can change the type of instability from static instability to dynamic instability. This is the physical mechanism of the stabilizing effect of rocket thrust.

Through consideration of the test columns and the stability maps, the present experiment is focused on demonstrating the following two cases.

Case 1: Initially, the column under a conservative load sways with a low frequency, since the load is closed to but lower than the buckling load. Then the rocket thrust of 40 kgf will be applied to the column. The column may oscillate with a higher frequency during the burning of the rocket motor. After the burn out of the motor, the column shall again sway with the low frequency.

Case 2: Initially, the column under the buckling load is at rest in a bent configuration. Then the rocket thrust of 40 kgf is applied to the column in addition to the conservative buckling load. The application of the rocket thrust may make the column dynamically stable as long as the thrust is alive. After the burn out, the column shall again have the bent configuration.

Figure 9 shows the sketch of the experimental set-up. A vertical column was cantilevered upward and equipped with a solid rocket motor at its tip end. The motor was loosely harnessed by two thin wires to prevent the column to sway out extremely, but allow it to

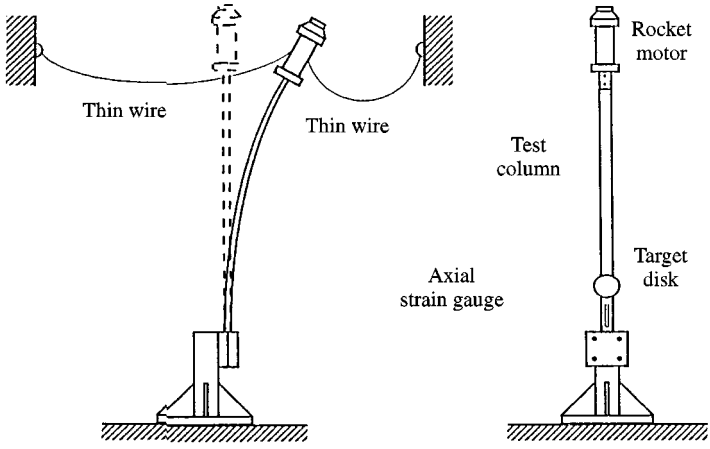

Figure 9. Conceptual sketch of experimental set-up.

oscillate freely with a small and moderate amplitude. Measuring devices were installed on the column for axial compressive strain and lateral displacement of the test columns. Dynamic behavior of the columns was recorded by a video camera and a motor driven camera. The photograph of the test column in the experimental set-up is shown in Figure 1.

It is again noted that the nominal weight of the motor before ignition was 14·65 kgf, while the weight of the propellant was 0·9 kgf. This means that the weight of the motor after burn out was 13·75 kgf. Thus, the average weight of the motor during burning was 14·2 kgf. The rocket thrust was assumed to be constant and of 40 kgf (392N) during the burning period of 4 s.

6.2. RESULTS OF THE EXPERIMENT

Four test runs were conducted in the present experiments.

Test run No. 1: The test column No. 1 was fixed vertically in the set-up. The length of the column is 1040 mm, the width 30 mm and the thickness 9 mm. The vertical column without rocket thrust swung with a low frequency and rather a large amplitude. Under the action of rocket thrust, it oscillated with a higher frequency and a smaller amplitude. After burn out of the rocket, it again swung as it was before ignition.

Test run No. 2: The test column No. 2 was on its service. The length of the column is 1130 mm, the width 30 mm and the thickness 9 mm. Since the test column of the run No. 2 had a longer length than that of No. 1, the former oscillated with a lower frequency than the latter. Recorded displacement and axial strain were shown in Figure 10. It was observed through Figure 10 that the column under a conservative load oscillated with a low frequency of 0·29 Hz (0·227 Hz predicted by equation (15)), while, under a rocket thrust in addition to the conservative load, it oscillated with a higher frequency of 0·66 Hz (0·544 Hz predicted by equation (15)). Experimental first eigenfrequencies before and after the application of the rocket thrust are plotted in Figure 11. Points A and B in Figure 11 represent the experimental values to be compared with the theoretical prediction.

Test run No. 3: The test column No. 3 was on duty. The dimensions of the column were $1330 \times 30 \times 9$ mm. The length of the test column was so determined that it was just slightly

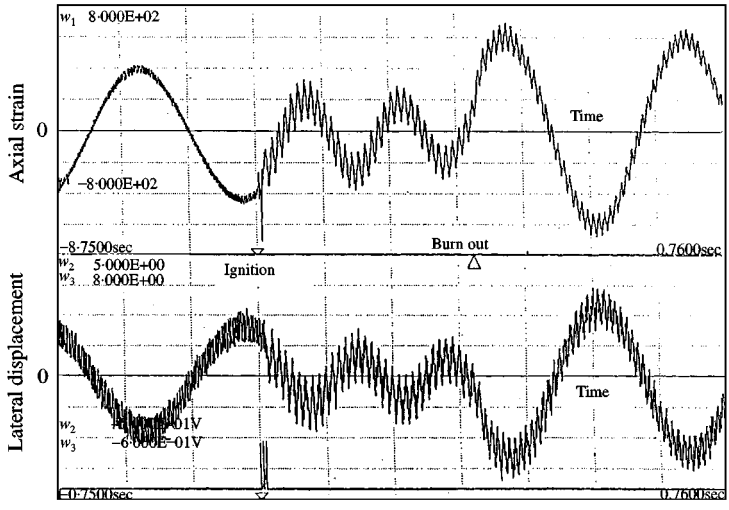

Figure 10. Recorded axial strain and displacement for the test run No. 2.

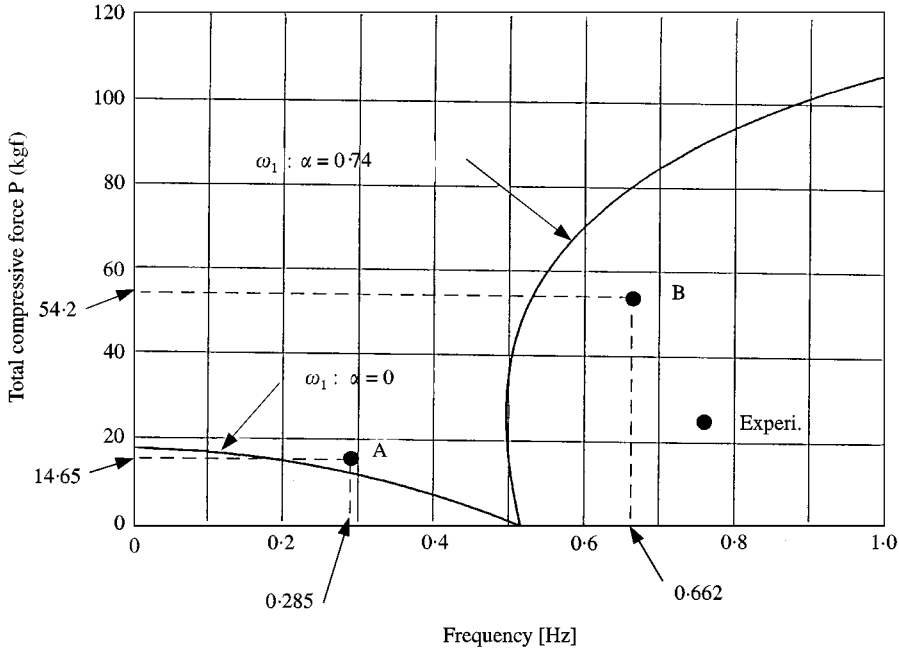

Figure 11. First eigenfrequency of the column in the test run No. 2.

longer than the critical length for buckling. Thus, the column without rocket thrust was in the state of bent configuration. Application of rocket thrust yielded the total compressive load of 54·2(14·2 + 40) kgf in average. At the moment of the application of rocket thrust, the bent column stood up and began to swing with a moderate frequency. After the burn out of the motor, the column swung with a very low frequency. The reason why the column could not retain its bent configuration was that all the propellant of 0·9 kgf was consumed out and thus the weight of the motor after the burn out was then 13·75 kgf.

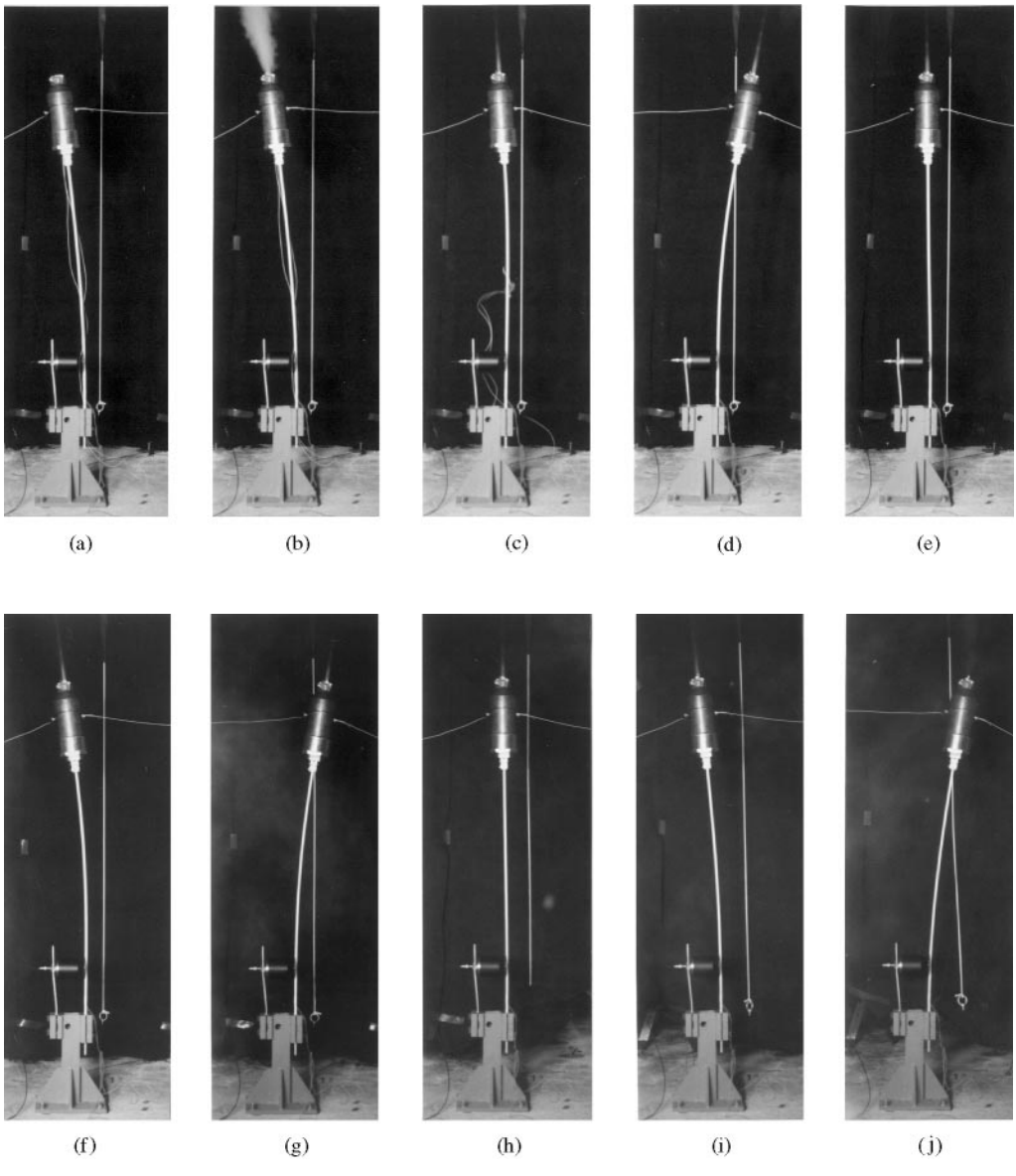

Figure 12. Sequence of frames of the column's behavior observed in the test run No. 4: (a) Before the ignition, bent column without rocket thrust; (b) $t = 0{\cdot}0$ s; Ignition; (c) $t = 0{\cdot}5$ s; (d) $t = 1{\cdot}0$ s; (e) $t = 1{\cdot}5$ s; (f) $t = 2{\cdot}0$ s; (g) $t = 2{\cdot}5$ s; (h) $t = 3{\cdot}0$ s; (i) $t = 3{\cdot}5$ s; (j) after a while after the burn out, bent column without rocket thrust.

Test run No. 4: The test column No. 4 served for the test. The dimensions of the column were $1125 \times 30 \times 8$ mm. The dimensions were chosen to realize the buckled state of the column. Under the combined action of the motor's weight and rocket thrust, i.e., $P = W + T = 54{\cdot}2$ kgf in average, the column oscillated with a moderate frequency around the undeformed configuration. After the burn out of the motor, the column retained its bent configuration.

A sequence of frames of the column's behavior observed in the test run No. 4 was shown in Figure 12. Figure 13 depicts the records of the axial strain and dynamic displacement in

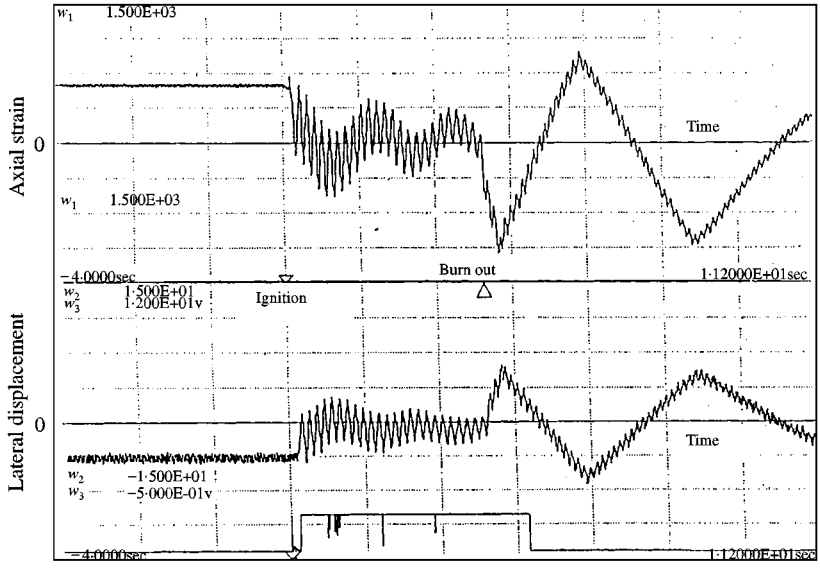

Figure 13. Recorded axial strain and displacement for the test run No. 4.

the test run No. 4. Figures 12 and 13 testify the stabilizing effect of rocket thrust on the dynamics of the column initially subjected to the conservative buckling load.

Now, it is worthwhile to explain the observed records in Figure 13, which shows the dynamic behavior of the test column No. 4 under a follower rocket thrust. Before the ignition and thus without the rocket follower force, the test column is buckled and in rest in its bent configuration. Between the ignition and the burn out, the column oscillated about its rectilinear form with finite frequencies. After the burn out, the column lost again its stability by divergence, in a linear divergent motion. Since the amplitude of the test column was constrained within a not extremely large amplitude by the harness wires in both sides as shown in Figures 1 and 9, the linear divergent motion in one side would soon be pulled back to the opposite side due to the elasticity of the stretched wire harness at the other side, and so on. In this way, the essentially divergent motion behaved as if the motion was a discontinuous relaxation oscillation. Finally, the relaxation motion, due to air resistance, settled in the buckled configuration as shown in Figure 12(j).

7. CONCLUDING REMARKS

The present paper has presented the experimental demonstrations of the stabilizing effect of rocket thrust on the dynamics of vertical cantilevered columns having a tip rigid body. As shown in the test runs Nos. 1 and 2, rocket thrust can cause the column's oscillation with a higher frequency than when it was subjected only to a conservative load. More dramatic demonstrations were made by the test runs Nos. 3 and 4, where the buckled column under a conservative load regained dynamically their straight configurations during the application of rocket thrust. The following main conclusions can be summarized;

(1) Sub-tangential force is a realistic force to be produced by the rocket thrust and the self-weight of the rocket motor mounted to a vertical cantilevered column at its tip end.

(2) In place of ideal Beck's column, a cantilevered column having a rigid body at its free end can be established as a realistic non-conservative elastic model.
(3) It was experimentally demonstrated that a buckled Euler column could be dynamically stabilized by the action of a tangential follower force.

REFERENCES

1. V. V. BOLOTIN 1963 *Nonconservative Problems of the Theory of Elastic Stability*. London: Pergamon Press.
2. D. J. MCGILL 1971 *Journal of the Engineering Mechanics Division, American Society of Civil Engineers* **97**, 629–635. Column instability under weight and follower loads.
3. Y. SUGIYAMA and H. KAWAGOE 1975 *Journal of Sound and Vibration* **38**, 341–355. Vibration and stability of elastic columns under the combined action of uniformly distributed vertical and tangential forces.
4. Z. CELEP 1977 *Zeitschrift fuer Angewandte Mathematik und Mechanik* **57**, 555–557. On the vibration and stability of Beck's column subjected to vertical and follower forces.
5. Y. SUGIYAMA and K. A. MLADENOV 1983 *Journal of Sound and Vibration* **88**, 447–457. Vibration and stability of elastic columns subjected to triangularly distributed sub-tangential forces.
6. B.-J. RYU and Y. SUGIYAMA 1994 *Computers and Structures* **51**, 331–335. Dynamic stability of cantilevered Timoshenko columns subjected to a rocket thrust.
7. Y. SUGIYAMA, K. KATAYAMA and S. KINOI 1995 *Journal of Aerospace Engineering* **8**, 9–15. Flutter of cantilevered column under rocket thrust.
8. Y. SUGIYAMA, J. MATSUIKE, B. J. RYU, K. KATAYAMA, S. KINOI and N. ENOMOTO 1995 *AIAA Journal* **33**, 499–503, **34**, 212. Effect of concentrated mass on stability of cantilevers under rocket thrust.
9. B.-J. RYU, K. KATAYAMA and Y. SUGIYAMA 1998 *Computers and Structures* **68**, 499–512. Dynamic stability of Timoshenko columns subjected to subtangential forces.
10. Y. SUGIYAMA, M. A. LANGTHJEM and B.-J. RYU 1999 *Journal of Sound and Vibration* **225**, 779–782. Realistic follower forces.